Hindawi
Journal of Chemistry
Volume 2019, Article ID 8184732, 13 pages
https://doi.org/10.1155/2019/8184732

Research Article

Eco-Friendly Photocatalyst Derived from Egg Shell Waste for Dye Degradation

Achala Amarasinghe[1] **and Dakshika Wanniarachchi**[2]

[1]*Department of Science and Technology, Uva Wellassa University, Badulla, Sri Lanka*
[2]*Instrument Center, Faculty of Applied Sciences, University of Sri Jayewardenepura, Nugegoda, Sri Lanka*

Correspondence should be addressed to Dakshika Wanniarachchi; dakshikacw@sjp.ac.lk

Received 14 June 2019; Revised 14 August 2019; Accepted 16 August 2019; Published 26 September 2019

Guest Editor: Hassan Ait Ahsaine

This study is focused on removal of dyes in water bodies using calcined egg shell powder obtained from waste egg shells as a new material for photocatalytic dye removal. The photocatalytic activity of calcined egg shell powder (CESP) was compared with the raw egg shell powder (RESP) under light and dark conditions. The results reveal that CESP has significantly a higher dye degradation capability of 80% compared to the RESP which is 20% under the same condition. Furthermore, under light conditions, CESP has shown nearly 50% increase in dye degradation compared to the same material in the dark. The kinetics of dye degradation follows pseudo-second-order kinetics suggesting the chemisorption process and the Freundlich adsorption isotherm is best fitted (R^2 value is 0.96 for the linear fit) with the dye adsorption process. The application of CESP in industry is studied with a textile acid dye Lanasyn Rez F5B, and the results reveal it follows pseudo-second-order kinetics in dye removal.

1. Introduction

Colour is a major parameter considered when defining the quality of water. Colour of water is often changed due to dissolved or suspended solids. Naturally, colour of water can be changed due to tannings from decomposing leaves or mud on a rainy day. However, water bodies are polluted because of the release of improperly treated industrial waste containing various dyes and pigments. These could prevent penetration of sunlight into the bottom of rivers and lakes causing a decrease in dissolved oxygen content and threat to aquatic plants and animals in threat. Furthermore, dyes and degraded by-products of dyes are toxic and carcinogenic [1, 2].

The removal methods available for textile dyes can be classified as physical methods, biological methods, and chemical methods [3]. Physical methods often consider adsorption of a dye on to a suitable sorbent. Here, activated carbon is the most efficient in removing variety of dyes [4]. However, it has limitation in application due to the high cost and material loss during regeneration [3]. Consequently, there are some low-cost sorbents introduced with biological origin as alternatives [4–8]. Apart from physical methods, biological treatments include use of algae or bacteria to metabolize decomposition of dyes. [9, 10]. Conversely, most of the dyes are designed to give a long-lasting colour to the textile. Therefore, degradation of these dyes requires advanced chemical oxidation methods. Some of the most studied and used oxidants are ozone [11] and hydrogen peroxide in the presence of UV light. The Fenton process is also used in degradation of textile dyes [12]. All these methods utilize highly reactive radical species of oxygen or hydroxyl to breakdown the dye [12–14]. However, these reactive oxygen species are short lived; hence, industrial application of hydrogen peroxide is limited. There are novel methods emerging in situ generation of hydrogen peroxide/hydroxyl radical for more viable use [12, 15]. Metal oxides such as titanium oxide [16–18] and zinc oxide [19, 20] are widely studied and used in degradation of dye materials photocatalytically. The inherent problems which limit the use of TiO_2 is the band gap which is ~3.2 eV and requires UV light to operate as a photocatalyst [21]. Studies are extended

to include composites of TiO_2 or ZnO with other metal oxides aiming higher degradation efficiency and photocatalytic activity using visible light [21–25].

There is constant search for novel photocatalysts other than traditional TiO_2- or ZnO-based catalysts. In recent years, there have been number of studies conducted on calcium-based photocatalysts such as calcium hydroxyapatite [26] and calcium antimony oxide hydroxide [27] for dye degradation. In addition, calcium hydroxide is also used as a catalyst for transesterification in biodiesel production [28]. Although there are many alternatives for calcium sources, egg shells can be utilized as it is available in abundant [29] and often considered as a waste material which is discarded without further use. The current trends to use egg shell waste are in agriculture as a fertilizer or as animal feed [30]. The anatomy of egg shell indicates the presence of pores which facilitate air exchange for the growing embryo [31]. Therefore, this material serves as an effective surface for dye adsorption processes. There have been studies conducted for the use of egg shell powder and egg shell membrane for dye removal [32–38]. Furthermore, egg shell powder has been used to develop several composite materials for dye removal incorporating TiO_2, polymer, and clay materials [39–42]. There is a significant enhancement in dye removal activity observed for egg shell powder composites compared to egg shell powder alone [39–42].

However, the dye removal capability of egg shell powder which is thermally treated above the thermal decomposition temperature (830°C) is not studied so far. Also, the photocatalytic activity is not well established for the calcined egg shell powder (CESP). Therefore, the main focus of this paper is to evaluate the dye removal efficiency of CESP as an adsorbent and as a photocatalyst. The term calcination is defined as the heating of a substance to high temperature allowing oxidation and release of any volatile substances [43]. In many papers, calcined egg shell powder indicates well purified and dried egg shell powder (100–120°C) [36]. However, in in this paper, the "calcined egg shell powder (CESP) denotes egg shell powder heated at 900°C which is above the decomposition temperature of calcium carbonate.

Dye removal efficiency and photocatalytic dye degradation of the two materials were compared using methylene blue as the model dye. The dye adsorption processes are studied with the Langmuir and Freundlich isotherms, and rates were evaluated as first-order and pseudo-second-order kinetics. Furthermore, dye removal capacity of textile acid dye Lanasyn F5B was studied as an application of the CESP in industrial dye removal.

2. Materials and Methods

2.1. Materials and Chemicals. Egg shells were obtained from the university cafeteria. Methylene blue (Merck limited, India) and industrial dye (Lanasyn Rez F5B) (Riddhi Siddhi Trading Co. Maharashtra, India) were purchased and used as received.

2.2. Calcined Egg Shell Powder Preparation. Egg shells were collected from the university cafeteria and cleaned with distilled water thoroughly to remove all the unnecessary materials adhered to the egg shells. Then, egg shells were dried at 120°C in the oven for 24 hours. Dried egg shells were ground and calcined in a muffle furnace (HD-230 "PAD," Forns Hobersal SL, Barcelona) under static air conditions at 900°C to produce CESP for 3 hrs.

2.3. Calcined Egg Shell Powder Characterization. Characterization of CESP and RESP was done by Fourier-transform infrared (FTIR, Brucker, Alpha) and X-ray diffraction (Rigaku Ultima IV) (S1.Tables 1–4 for supporting information regarding experimental conditions).

2.4. Photocatalytic Experiments. The photocatalytic activity of CESP and RESP was compared by evaluating dye removal efficiencies of solutions with dye and egg shell powder under the dark and light conditions. The removal efficiency of calcined egg shell powder and raw egg shell powder was calculated by taking 0.50 g of each powder dispersed in MB solutions (50 ml, 10 mg/l) in a glass stoppered bottle. Then, for each type of powder, one solution was kept under light condition, while the other solution was kept under dark condition for 2 hrs. Light condition was provided by 23 W of fluorescent bulb inside a light box. Solutions were centrifuged, and absorbance was measured using the UV-visible spectrophotometer (GENESYS, Thermo Scientific) every 30 minutes. Each experiment was conducted in triplicate. Removal efficiency was calculated by using equation (1). Removal efficacies were repeated for CESP under light conditions in triplicate and in the dark for two hours and 9 hrs. RESP study was repeated for 2 hrs and 9 hrs duration (S2.Tables 1 and 2 and S3.Tables 1 and 2 and S3.Figures 1 and 2 for supporting information regarding experimental conditions):

$$\eta = \frac{(C_0 - C_f)}{C_0} * 100, \quad (1)$$

where η is the removal efficiency, C_0 is the initial MB concentration (mg/l), and C_f is the MB concentration at equilibrium (mg/l).

2.5. Adsorption Experiments. Adsorption studies were conducted for CESP (0.50 g) placed in a glass stoppered bottle with 50 ml solutions of MB aqueous solutions (4 mg/l, 6 mg/l, 8 mg/l, 10 mg/l, 12 mg/l, 14 mg/l, 16 mg/l, 18 mg/l, and 20 mg/l). These solutions were studied under the light conditions. Then, absorbance measurement of each solution was obtained after 28 hrs. Amount of dye adsorbed and degraded at the equilibrium (q_e) was calculated by equation (2) for Langmuir and Freundlich isotherms. A control experiment was conducted in parallel without the CESP. Experiment was repeated twice:

$$q_e = \frac{(C_0 - C_e) * V}{W}, \quad (2)$$

where q_e is the amount of MB adsorbed at the equilibrium (mg/g), C_0 is the initial MB concentration (mg/l), C_e is the

MB concentration at equilibrium (mg/l), V is the volume of the solution (L), and W is the mass of the dry adsorbent (g) (S4.Figures 1–4 for supporting information regarding repeated trials for isotherms fitting):

2.6. Kinetic Studies. CESP (0.50 g) was dispersed in MB solution (10 mg/l, 50 ml). One solution was used as the control without exposing to light by covering it with an aluminium foil. All samples were kept under the 23 W fluorescent bulb for 2 hrs inside the light box. Absorbance of each sample was measured at 15-minute intervals. The amount of MB adsorbed from the solutions at various time intervals was calculated by equation (3). Same procedure was followed for RESP. The experiment was conducted in triplicate:

$$q_t = \frac{(C_0 - C_t) * V}{W}, \quad (3)$$

where q_t is the amount of MB adsorption at time t (mg/g), C_0 is the initial MB concentration (mg/l), C_t is the concentration of MB at any time t (mg/l), V is the volume of the solution (L), and W is the dry mass of the adsorbent (g).

2.7. Removal Efficiency of Industrial Dye. The removal efficiency of industrial dye was studied using 50 mg/l, 60 mg/l, 70 mg/l, 80 mg/l, 90 mg/l, and 100 mg/l of industrial dye solutions. Maximum absorbance wavelength of the industrial dye was 530 nm. Adsorption isotherms were developed using 1.5 g of CESP dispersed in 25 ml of 50 mg/l, 60 mg/l, 70 mg/l, 80 mg/l, 90 mg/l, and 100 mg/l dye solutions. Then, absorbance of these solutions was measured after keeping them under the light condition for 28 hours to calculate q_e. Kinetic experiments were conducted for 25 ml of 100 mg/l industrial dye solutions with 1.5 g of CESP. These solutions were kept under light for 2 hours, and absorbance of samples was measured for every 15 minutes.

3. Results and Discussion

3.1. Sample Characterization. According to the data of XRD illustrated in Figures 1(a) and 1(b), crystalline calcite in RESP and calcium hydroxide in CESP are present. Therefore, it is clear that calcium carbonate in raw egg shell powder has been transformed into the calcium oxide at 900°C. But due to exposure to the atmosphere, it is converted to calcium hydroxide. The presence of narrower peaks indicates that CESP and RESP are crystalline. The size of the crystallite is calculated using Debye–Scherrer's formula [44] considering crystals spherical with cubic symmetry ($K = 0.94$) for Cu-Kα wavelength (1.5406 Å) for peak between 2Θ values 30 deg. to 60 deg.

Accordingly, the average crystallite size of RESP is about 30–45 nm and that of CESP is about 15–23 nm.

Tsai et al [45] have characterized RESP with FTIR spectroscopy. The FTIR spectrum of RESP (Figure 2) indicates presence of organic matter corresponding to C-H vibration peaks at 2969 cm^{-1}, 2875 cm^{-1}, and 2527 cm^{-1}. These FTIR bands are absent in egg shell powder calcined at 900°C, indicating decay of organic matter. The peak at 1416 cm^{-1}, 879 cm^{-1}, and 705 cm^{-1} is related to the carbonate anion [45, 46]. Furthermore, the band at 515 cm^{-1} for CESP indicate the OH band and for the calcium oxide band. According to the XRD data and FTIR data, further confirmation is provided for the transformation of calcium oxide to calcium hydroxide.

3.2. Comparison of Removal Efficiencies and Photocatalytic Activity. The removal efficiencies of MB were studied with raw egg shell powder and calcined egg shell powder recording UV-Visible spectra every 30 minutes under dark conditions. The UV-visible spectrum of MB clearly indicates a decrease of the band at 665 nm as MB is adsorbed into egg shell powder, as illustrated in Figures 3(a) and 3(b).

Figures 3(a) and 3(b) represent the absorbance curves of MB due to RESP and CESP, respectively. MB concentration of both solutions has been reduced gradually within 2 hours. But absorbance curves of MB solution with CESP indicate blue shift of the band at around 560 nm after 75 minutes. But this is absent in the solution of MB-RESP, and only reducing absorbance curve is observed. If only adsorption is the process which was proceeding in the experiment, reducing curves must be generated without any movement of curves. This suggests another reaction is the reason for the shifting of this curves.

Egg shell is designed by nature to give protection to the embryo from harmful attacks of bacteria other factors. A thin layer of the protein matrix is bonded to the egg shell containing calcite. The egg shell has many pores to allow exchange of gaseous products and water for healthy growth of the embryo [31]. Therefore, decrease in MB concentration in solution observed in raw egg shell powder and calcined egg shell powder under dark could be due to physical adsorption, which is in accordance with the work of Tsai and coworkers [32, 45]. Furthermore, the work of El-Kemary and coworkers on TiO_2/egg shell nanocrystals reported increasing removal efficiency when the calcination temperature is increased from 400°C to 900°C for the acid red nylon 57 dye [39]. Therefore, the enhanced dye degradation of CESP compared to RESP is in agreement with the above data.

The photocatalytic activity was studied for RESP and for CESP. Figures 4(a) and 4(b) indicate the absorbance curve of MB solutions with RESP and CESP in the presence of visible light. Figure 4(b) clearly indicates a degradation reaction proceeding in the solution with CESP. In the presence of light, even at the beginning, the absorbance curve has been blue shifted. But these changes are not observed in the solution with the RESP. Only deducing curves can be observed. The solution with CESP indicates reduction of MB concentration, and bands of the absorbance curves after 105 minutes have been changed significantly, shifting the maximum absorbance towards 615 nm. However, Figure 3(b) (dark condition) indicates small shifting of curves with comparison to Figure 4(b) (light condition). Studies of Yang et al. on photocatalytic degradation of MB with the rice husk/TiO_2/SiO_2 catalyst observed rapid degradation of MB in the presence of visible light [47].

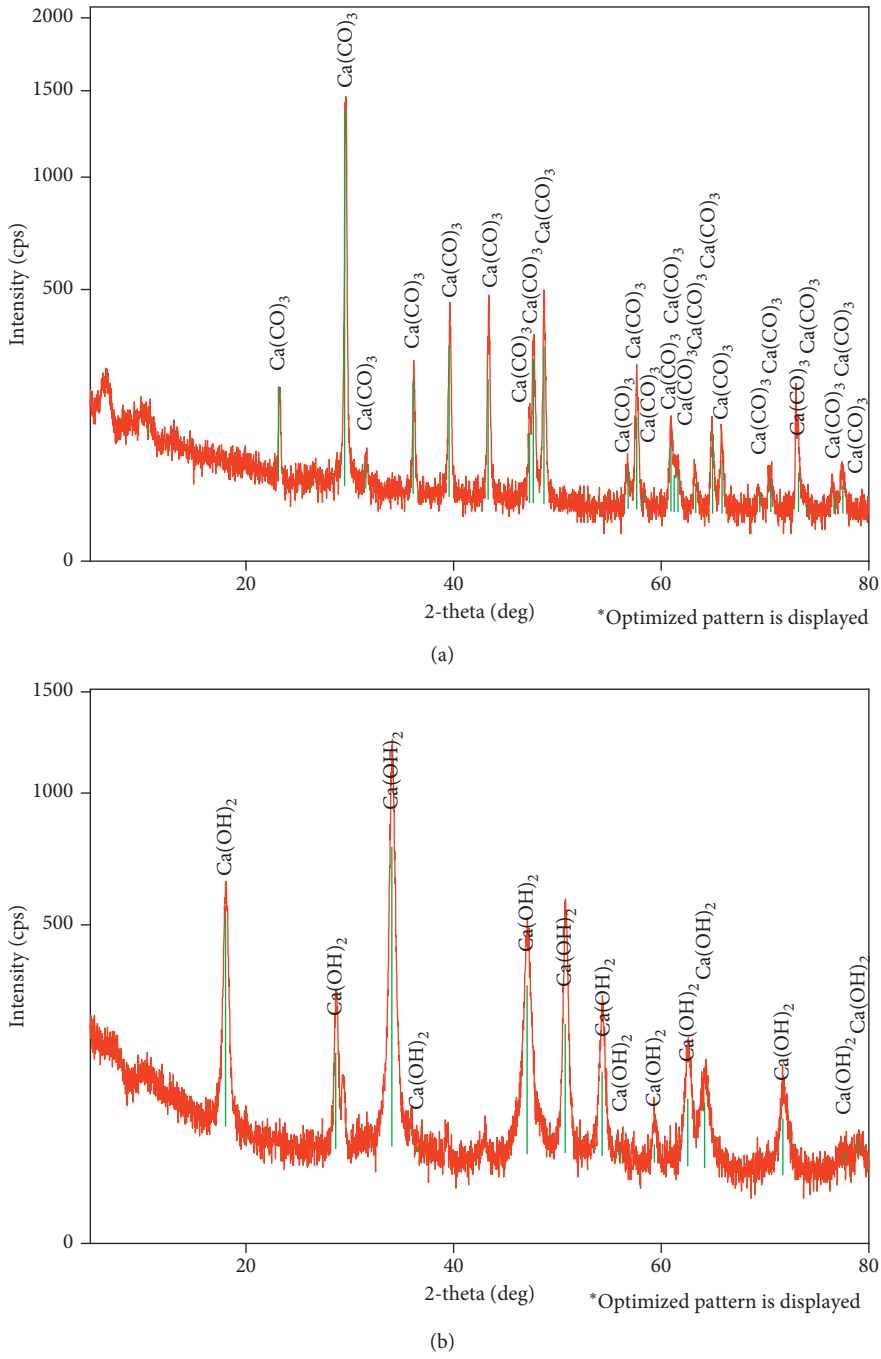

Figure 1: X-ray diffraction patterns: (a) raw egg shell powder; (b) calcined egg shell powder.

CESP mainly consists of $Ca(OH)_2$ which can give basic solution when dissolved in water. Hence, it can be presumed that the reason for the alteration of adsorption bands could be due to the basicity. In order to clarify this fact, absorbance curves of MB solution were measured with different pH values. Figure 5 interprets the absorbance curves of MB at different pH values. The pH value of solutions is adjusted with using HCl and NaOH solutions. According to Figure 5, it is clear that pH alone is not the agent for shift in UV-visible bands in MB solution. However, the pH of the solution is an important factor which decides the surface potential of the material. In a study where TiO_2 is used as the photocatalyst, it is observed that the dye adsorption and degradation are enhanced in a higher pH value. This is due to the availability of the anionic surface (TiO^- in this case) to bond with the -C-S^+=C- group in MB to initiate degradation of MB producing the sulfone group [48]. Therefore, possibly a similar phenomenon can be suggested for the CESP.

Removal efficiency of MB was calculated for both RESP and for CESP. Figures 6(a) and 6(b) compare the removal efficiencies of MB under dark and light conditions for both types of egg shell powders. In the presence of light, removal

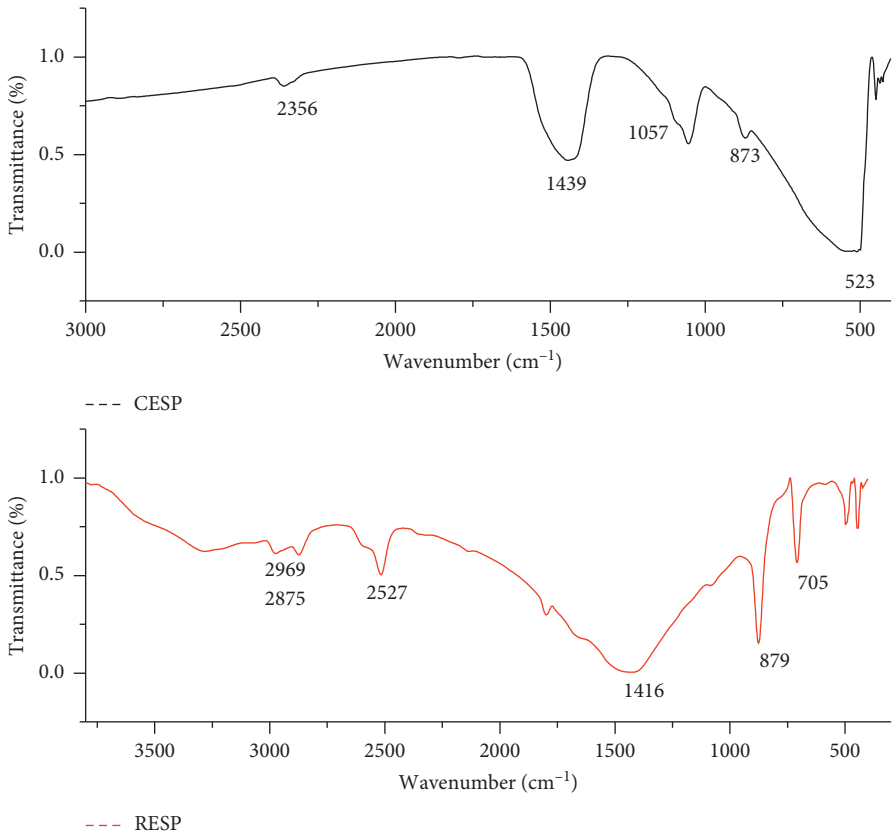

Figure 2: FTIR spectra of raw egg shell powder and calcined egg shell powder.

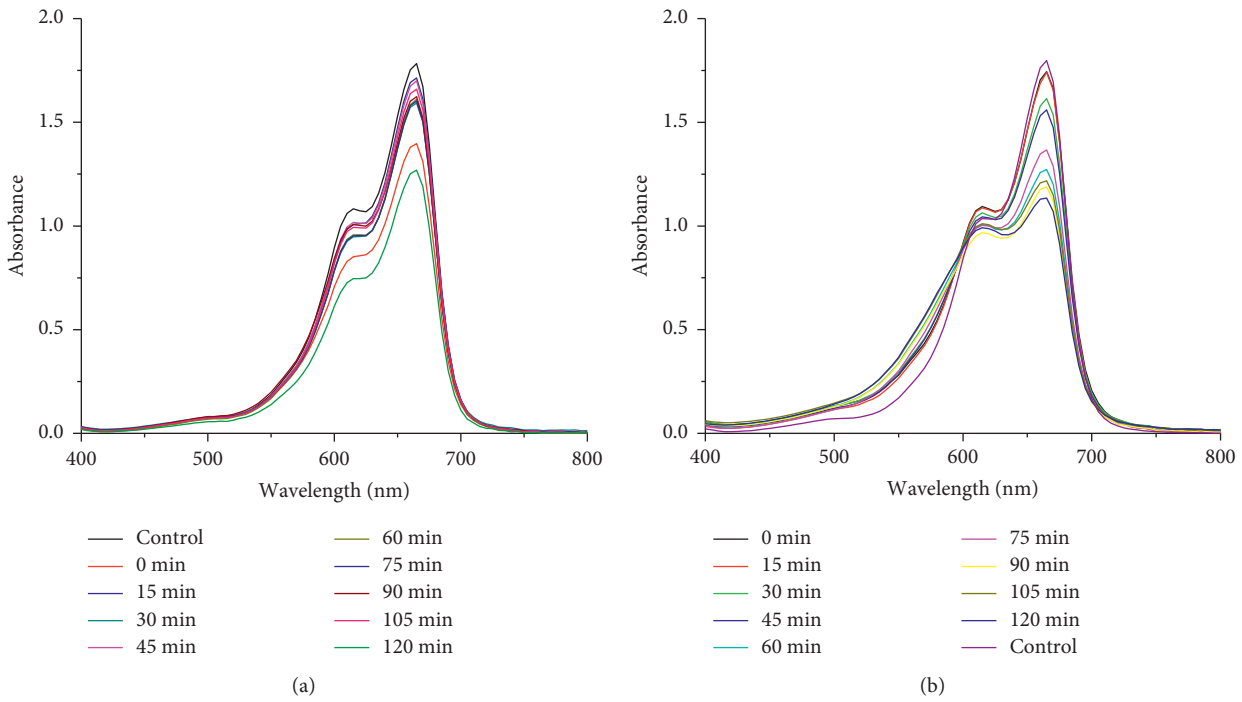

Figure 3: Absorbance curves of MB solution (dark): (a) raw egg shell powder; (b) calcined egg shell powder.

efficiency of CESP is higher than RESP. The reported efficiency for CESP after 2 hours is 82%, while that of RESP is 21%. Comparatively, CESP has higher removal efficiency than RESP under light conditions. Furthermore, when CESP considered, the removal efficiency in the presence of light (82%) is much higher than that in the dark (44%). These

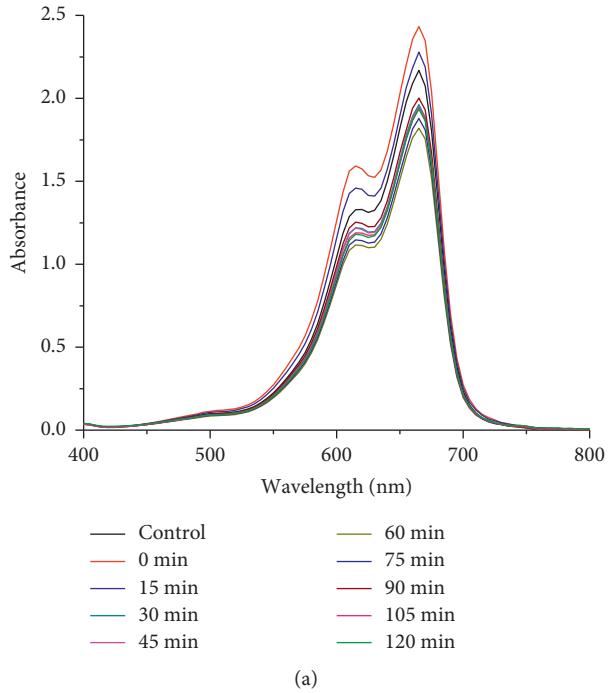

(a)

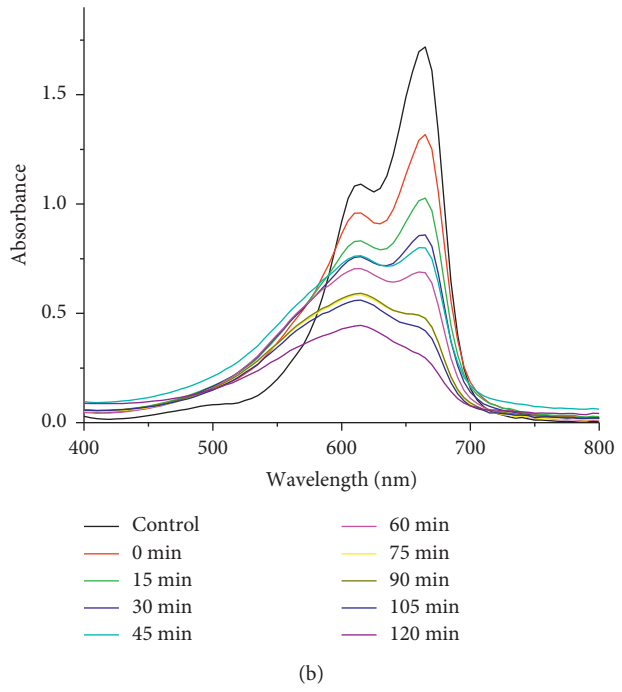

(b)

Figure 4: Absorbance curves of MB solution (light): (a) raw egg shell powder; (b) calcined egg shell powder.

figures clearly interpreted that removal efficiency of MB in the light condition is higher compared to the removal efficiency in the dark condition. The calculated removal efficiencies under dark and light conditions are given in S2.Tables 1 and 2 in the supporting information, respectively.

The removal efficiencies were calculated with standard deviation between 10 and 5%. This suggests a possible degradation pathway involving photocatalytic activity. The semiconductor materials absorb photons from the UV radiation and promote electrons in the valence band to the

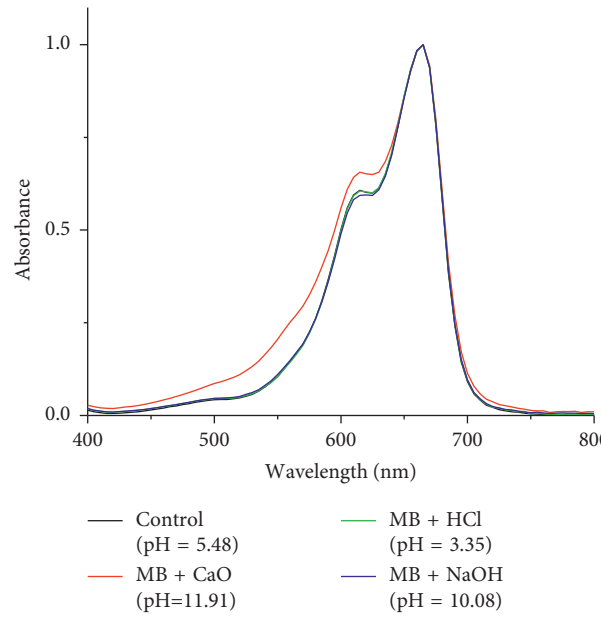

Figure 5: Absorbance curves of MB solution in different pH values.

conduction band, creating a hole in the valence band. These excited electrons can react with dye or oxygen to produce the superoxide anion. At the same time, holes in the valence band can also react with water molecules to produce hydroxyl radical. Consequently, the presence of reactive oxygen species leads to degradation of dye [17]. RESP consists of mainly $CaCO_3$, and CESP has $Ca(OH)_2$. The reported band gap of these materials is 5.07 eV [29] and 5.7 eV [49, 50], respectively. These band gaps suggest photocatalytic activity under visible light conditions is hardly possible. However, studies of Zang et al. suggest observed band gap for $Ca(OH)_2$ is further reduced to 3.2 eV subtracting energy gap between bottom of the conduction band to the Fermi level (2.5 eV) from the band gap of conduction and valence (5.7 eV) [49]. This allows excitation wavelength around 400 nm; thus, catalyst could be active at the margin of visible radiation.

When photo is excited, MB is converted to cationic dye radical which degrades the by-products. The absorption bands at 665 nm and 615 nm of MB correspond to monomer and dimer units [51, 52]. The decrease in band at 665 nm in the presence of light with calcined egg shell powder suggests rapid degradation of monomer units. In addition, the blue shift observed is due to further degradation of phenothiazine [51]. Furthermore, the study using CESP was continued for more than 9 hrs, and the results reveal over 90% efficiency of MB removal under light conditions end of first 180 min, while it was only 65% under dark conditions. The recorded UV-visible spectra for long exposure study under light and dark conditions are given under supporting information S3.Figures 1 and 2. The efficiencies and maximum amount removed (q_{max}) are given in S3.Tables 1 and 2, respectively.

3.3. Kinetic Experiments for CESP and RESP. The kinetic behaviour of the dye degradation was studied with pseudo-first-order and pseudo-second-order kinetics to evaluate the

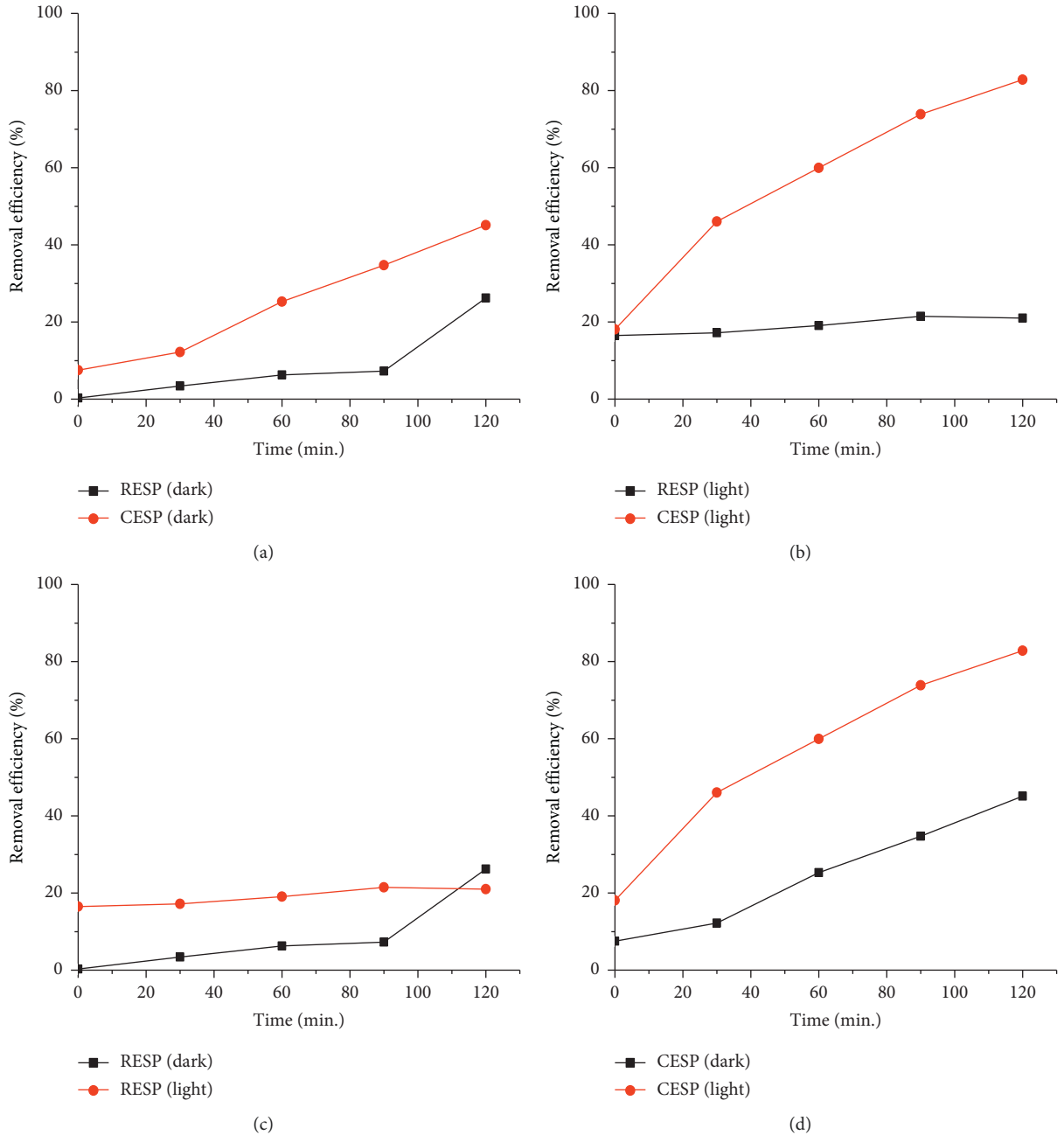

Figure 6: Removal efficiencies of MB in raw egg shell powder and calcined egg shell powder.

photocatalytic effect. The first-order and second-order kinetic models are given in equations (4) and (5).

First-order kinetic model equation [53]:

$$\frac{1}{q_t} = \frac{1}{q_1} + \frac{k_1}{q_1}\left[\frac{1}{t}\right], \tag{4}$$

where q_t and q_1 are the amount of dye adsorbed at time t and at equilibrium (mg/g) and k_1 is the first-order kinetic rate constant.

Second-order kinetic model [53]:

$$\frac{t}{q_t} = \frac{1}{k_2 q_2^2} + \frac{1}{q_2}t, \tag{5}$$

where q_2 is the maximum adsorption capacity, q_t is the adsorbed amount at time t (mg·g^{-1}), and k_2 is the equilibrium rate constant for pseudo-second-order kinetic (g mg^{-1}·min^{-1}).

Kinetic modes for MB on to the CESP are shown in Figures 7(a) and 7(b). When correlation coefficient values of pseudo-first-order and pseudo-second-order are compared, the R^2 value of pseudo-second-order is higher than the pseudo-first-order value. Therefore, pseudo-second-order kinetic is the best fitted kinetic model for MB on to the CESP. The kinetic study was conducted for the RESP in the same way, and RESP also follows pseudo-second-order kinetic model which is in agreement with Tsai and coworkers [32, 45] for MB adsorption on to egg shell powder. Since

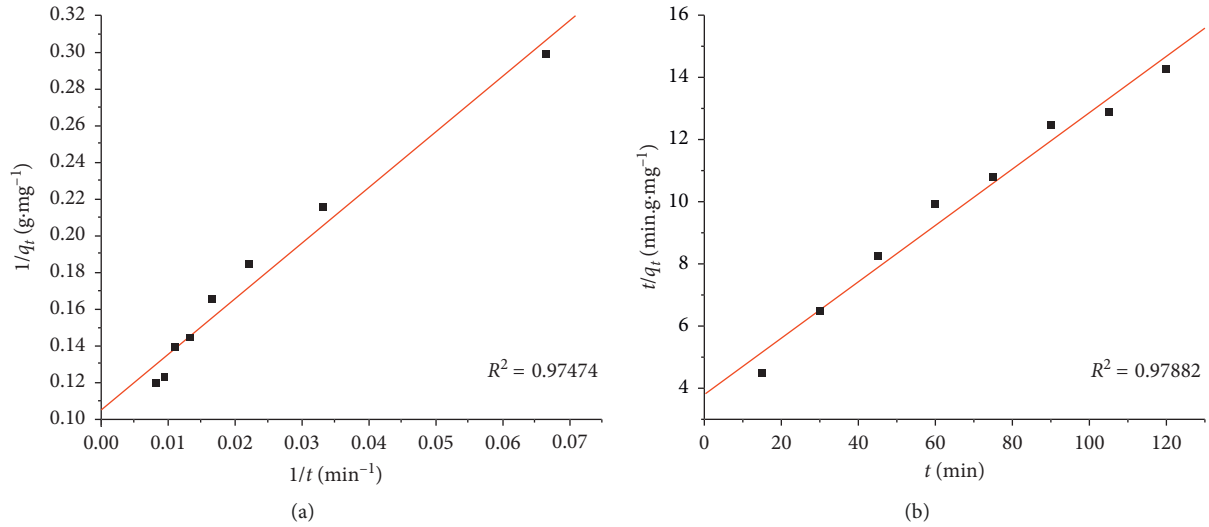

Figure 7: (a) First-order kinetics; (b) pseudo-second-order kinetics.

both CESP and RESP indicate pseudo-second-order kinetics, it is possible that the rate limiting step could be bimolecular and chemisorption governs the adsorption process [54] According to the results, CESP has higher adsorption capacity (11.025 mg·g^{-1}) compared to the RESP (0.23 mg·g^{-1}). Table 1 provides comparison of kinetic study for both types of powders.

3.4. Adsorption Isotherms for Calcined Egg Shell Powder. The adsorption capacities of MB on to CESP were evaluated using the Freundlich isotherm and Langmuir isotherm [53]. The linear forms of these isotherms are given in equations (6) and (7).

Langmuir isotherm:

$$\frac{C_e}{q_e} = \frac{1}{q_{\max} K_L} + \frac{C_e}{q_{\max}}, \quad (6)$$

where q_e is the equilibrium concentration on the calcium oxide (mg/g), C_e is the equilibrium concentration in the solution (mg/l), $q_{\max}$ is the monolayer adsorption capacity of the calcined egg shell powder, and K_L is the Langmuir constant (l/mg).

Freundlich isotherm:

$$\log q_e = \log K_f + \frac{1}{n} \log C_e, \quad (7)$$

where q_e is the equilibrium concentration on the calcium oxide (mg/g), C_e is the equilibrium concentration in the solution (mg/l), and K_f (l/g) and n are Freundlich constants.

According to Figures 8(a) and 8(b), Freundlich isotherm has a high R^2 value than the Langmuir isotherm. Therefore, the Freundlich isotherm is fitted better than the Langmuir isotherm. When Freundlich constant n gets some value other than 1, it gives a parabolic shape for the Freundlich isotherm. The value of n observed for calcined egg shell powder is one, suggesting a linear adsorption of the dye. These linear Freundlich graphs are vital in the industrial applications because linear adsorption provides direct applications for water treatment industries via direct calculations. Linear adsorption Freundlich graph can be used for calculation of dosage of adsorbent that should be added for maximum removal of the dye from the solution. Furthermore, the Freundlich adsorption isotherm suggests monolayer adsorption of the dye on the surface of calcined egg shell powder, thus facilitating the photocatalytic activity. Tsai and coworkers have studied the adsorption isotherm models for raw egg shell powder with MB. They have observed that the Freundlich isotherms fit more than Langmuir isotherms similar to the results obtained here [32, 45].

3.5. Removal of Industrial Dye Using Calcined Egg Shell Powder. Lanasyn F5B is an acid dye widely used in textile industry. The UV-visible spectra of the industrial dye and removal efficiencies at different time periods are given in S5.Figure 1 and S5.Table 1. The removal this dye using CESP was studied constructing adsorption isotherms and kinetic studies. According to Figure 9, the industrial dye does not a follow linear adsorption with Langmuir isotherm or Freundlich isotherm. The Freundlich adsorption isotherm constant (K_F) for the Lanasyn F5B dye is 0.058 Lg^1, and the Freundlich adsorption isotherm constant (n) is calculated as 0.985. The linear fit for the Freundlich adsorption isotherm is 0.6017 for R^2 suggesting the multilayer adsorption process may proceed with CESP. The industrial dye can be removed with more than 70% efficiency photocatalytically by CESP (S5.Figure 2).

Kinetic studies on this dye removal follow pseudo-second-order kinetics, as illustrated in Figure 9(d), which is comparable to the pseudo-second-order kinetics observed for MB adsorption with CESP. Table 2 provides a summary of adsorption isotherm data and results of kinetic experiments conducted for industrial dye using CESP.

3.6. Comparison of Use of Egg Shell Powder for Removal of Dye. Egg powder has been used to remove several well-known dyes. The studies have been conducted to evaluate

Table 1: Summary of kinetic studies for MB removal.

	First-order kinetics			Pseudo-second-order kinetics		
	k_1 (min^{-1})	q_e (mg·g^{-1})	R^2	k_2 (g·mg^{-1}·min^{-1})	q_e (mg·g^{-1})	R^2
RESP	5.97	0.22	0.63627	0.67	0.23	0.98451
CESP	0.0036	9.53	0.97474	0.0021	11.025	0.97882

Initial MB concentration = 10 mg/l; amount of CESP = 0.5 g.

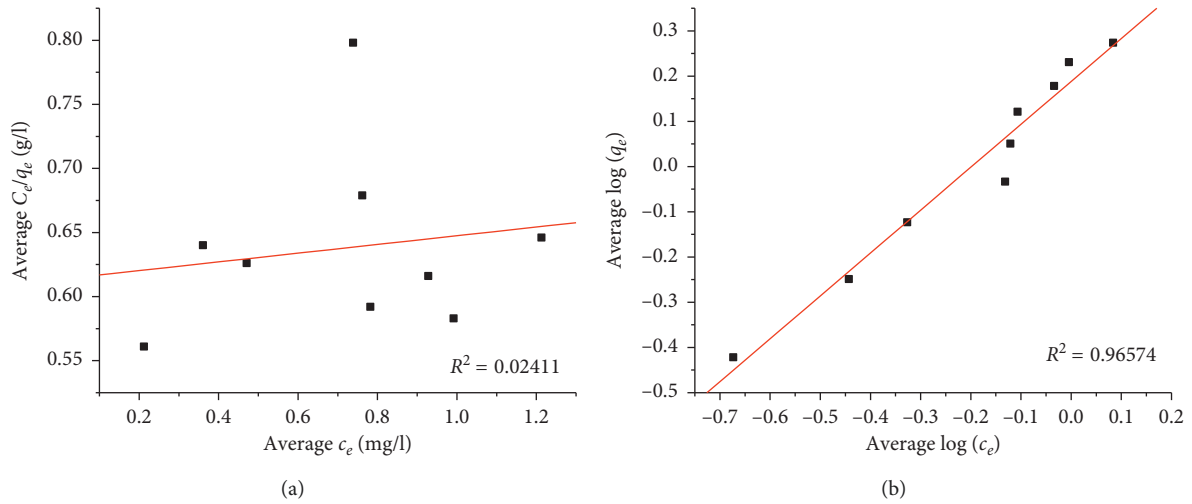

Figure 8: (a) Langmuir isotherm and (b) Freundlich isotherm for MB adsorption on to CESP.

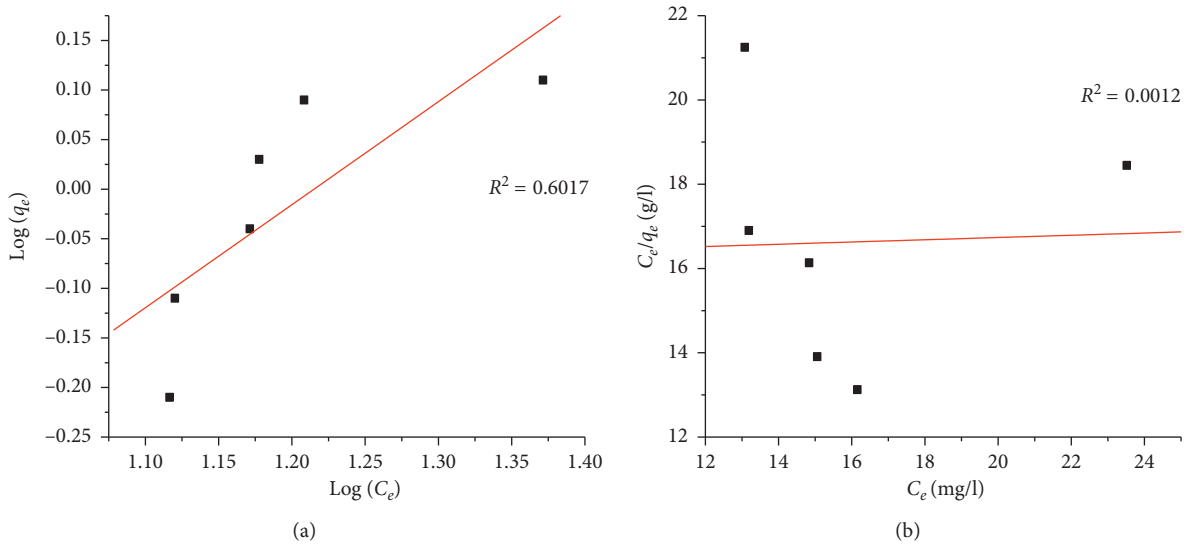

Figure 9: Continued.

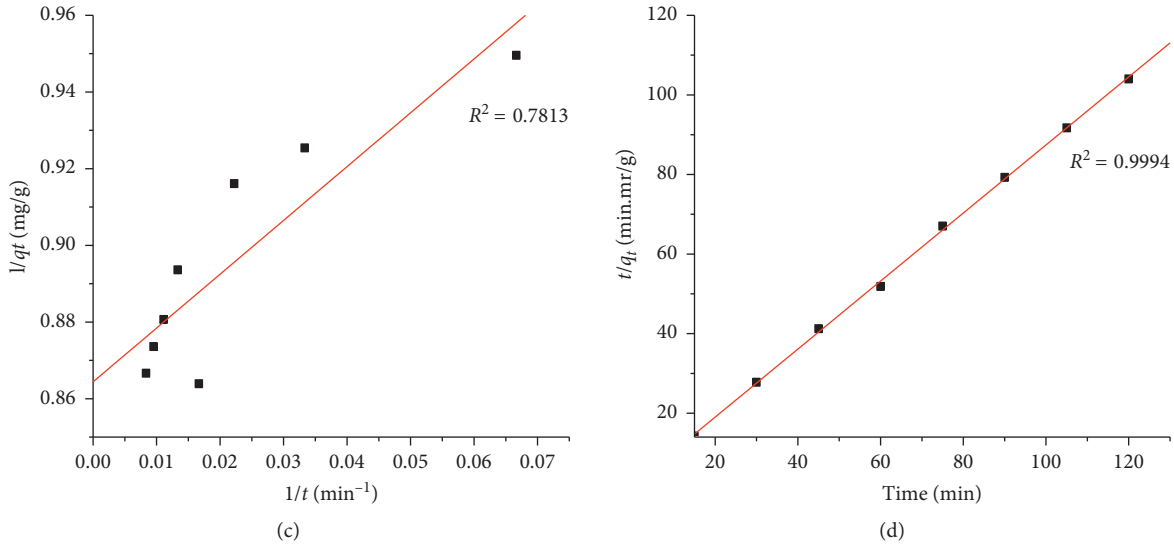

Figure 9: (a) Freundlich isotherm; (b) Langmuir isotherm; (c) pseudo-first-order kinetics; (d) pseudo-second-order kinetics.

Table 2: Results of kinetic experiments conducted for industrial dye using calcined egg shell powder.

	First-order kinetics			Pseudo-second-order kinetics		
	k_1 (min^{-1})	q_e (mg·g^{-1})	R^2	k_2 (g·mg^{-1}·min^{-1})	q_e (mg·g^{-1})	R^2
CESP	1.6241	1.1569	0.7813	0.2933	1.1777	0.9994

Initial MB concentration = 100 mg/l; amount of CESP = 1.5 g.

Table 3: Comparison of egg shell powder-, egg shell membrane-, and egg shell powder-based composite materials for dye adsorption.

Adsorbent	Dye	Adsorption capacity (mg/g)	Reference
Egg shell powder	Methylene blue	0.87	[35]
Egg shell powder	Methylene blue	0.8	[45]
Egg shell powder (RESP)	Methylene blue	**0.23**	This study
Egg shell powder (CESP)	Methylene blue	**11.02**	This study
Egg shell powder	Congo red	95.25	[33]
Egg shell powder	Rhodamine B	0.14	[34]
Egg shell powder	Rhodamine B	1.99601	[36]
Egg shell powder	Congo red	1.22	[35]
Egg shell powder	Bromophenol blue	0.04	[35]
Egg shell powder	Malachite green	2.13	[35]
Egg shell powder	Murexide	1.03092	[36]
Egg shell powder	Eriochrome black T	1.56494	[36]
Egg shell powder	Reactive red 123 dye (RR123)	1.26	[37]
Egg shell membrane and egg shell powder	C.I. Reactive yellow 205, a sulphonated reactive azo dye,	48.78	[38]
Egg shell membrane and egg shell powder	Rhodamine B	0.72	[34]
Egg shell membrane	Rhodamine B	14.4	[34]
Egg shell powder/TiO_2(TiO_2/CES)	Acid red nylon 57 (AN57)	220.2	[39]
Egg shell powder/polymer mixture of alginate and polyvinyl alcohol (biocomposite adsorbent)	C.I. Remazol reactive red 198	46.9	[40]
Calcined eggshell powder/anthill clay composite	Methylene blue	43.46	[41]
CaO photocatalyst	Indigo carmine dye	~100% dye degradation (approx. 1 hr exposure)	[44]
CESP photocatalyst	Methylene blue	80% degradation (approx. 1 hr exposure)	This study

dye removal capacity considering egg shell powder, egg shell membrane, and mixture of both components. In addition, there are several composite materials developed utilizing egg shell powder. Table 3 provides a comparison of performance of egg shell power in dye removal. In general, egg shell powder has a higher affinity for the anionic dyes compared to the cationic dyes. The MB adsorption on to CESP in this study is higher than the previously reported value for egg shell powders. Furthermore, recent studies on composite materials developed with egg shell powder indicate better removal capacity.

The photocatalytic ability of CaO was compared with TiO_2 by the work of Madhusudhana and coworkers for Violet GL2B azo dye and found that CaO is a more efficient catalyst compared to TiO_2 at high pH values. [55]. In another study, indigo carmine dye degradation was studied with CaO [44]. Table 3 provides a summary of utilizing egg shell-based materials for dye removal applications.

4. Conclusions

Egg shells are waste materials often without any reuse. Therefore, this study focused on how waste egg shell can be converted to a photocatalyst to remove toxic dye material. The two materials, raw egg shell powder (RESP) and calcined egg shell powder (CESP), have been compared for the dye removal efficiency under light and dark conditions. The enhanced dye degradation efficiency is observed with CESP in the presence of light compared to RESP suggesting it is a photocatalytic effect. The pseudo-second-order kinetic studies conducted for the RESP and CESP suggest MB is chemisorbed on the material. The equilibrium amount of dye adsorbed on the CESP is higher compared to RESP. The adsorption process best fitted with the Freundlich isotherm, suggesting monolayer of MB is adsorbed on to RESP and CESP. Furthermore, the CESP can be used to remove industrial dye Lanasyn F5B with 1.17 mg/g equilibrium dye adsorption capacity. In conclusion, the CESP has enhanced performance for dye degradation compared to RESP, highlighting its potential use as a novel and eco-friendly photocatalyst for dye degradation.

Data Availability

Data relevant for XRD studies and efficiency calculation are included in the supporting information. If further data related to analysis are required, the corresponding author can provide upon request.

Conflicts of Interest

The authors declare that there are no conflicts of interest.

Acknowledgments

The authors thank Department Science and Technology; Department of Animal Science, Uva Wellassa University; and Instrument Center, Faculty of Applied Sciences, University of Sri Jayewardenepura, for providing facilities for this study. Dr. Thusitha Etampawala is acknowledged for the discussions regarding XRD studies. The authors also thank Uva Wellassa University for the funding under grant UWU/R/G/2015/18.

Supplementary Materials

S1.Table 1: measurement conditions—raw egg shell powder (RESP). S1.Table 2: qualitative analysis results—raw egg shell powder and peak list (RESP). S1.Table 3: measurement conditions of calcined egg shell (CESP). S1.Table 4: qualitative analysis results of calcined egg shell and peak list (CESP). S2.Table 1: removal efficiency of RESP and CESP in dark condition. S2.Table 2: removal efficiency of RESP and CESP in light condition. S3.Figure 1: long exposure of MB on to the CESP in the light condition. S3.Figure 2: long exposure of MB on to CESP in dark condition. S3.Table 1: data of absorbance, equilibrium concentration, and equilibrium concentration of dye on the CESP and removal efficiency (dark). S3.Table 2: removal efficiency data of long exposure of MB with CESP powder (light). S4.Figure 1: adsorption isotherm trial for CESP. S5.Figure 1: UV-visible spectra of industrial dye. S5.Table 1: removal efficiency of industrial dye with CESP. S5.Figure 2: removal efficiency of industrial dye with CESP. (*Supplementary Materials*)

References

[1] C. A. Gonzales, E. Riboli, and G. Lopez-Abente, "Bladder cancer among workers in the textile industry: results of a Spanish case-control study," *American Journal of Industrial Medicine*, vol. 14, no. 6, pp. 673–680, 1988.

[2] Z. Singh and P. Chadha, "Textile industry and occupational cancer," *Journal of Occupational Medicine and Toxicology*, vol. 11, no. 1, p. 39, 2016.

[3] T. Robinson, G. McMullan, R. Marchant, and P. Nigam, "Remediation of dyes in textile effluent: a critical review on current treatment technologies with a proposed alternative," *Bioresource Technology*, vol. 77, no. 3, pp. 247–255, 2001.

[4] N. Kannan and M. M. Sundaram, "Kinetics and mechanism of removal of methylene blue by adsorption on various carbons-a comparative study," *Dyes and Pigments*, vol. 51, no. 1, pp. 25–40, 2001.

[5] T. Robinson, B. Chandran, and P. Nigam, "Removal of dyes from a synthetic textile dye effluent by biosorption on apple pomace and wheat straw," *Water Research*, vol. 36, no. 11, pp. 2824–2830, 2002.

[6] U. J. Etim, S. A. Umoren, and U. M. Eduok, "Coconut coir dust as a low cost adsorbent for the removal of cationic dye from aqueous solution," *Journal of Saudi Chemical Society*, vol. 20, pp. S67–S76, 2016.

[7] A. M. Aljeboree, A. N. Alshirifi, and A. F. Alkaim, "Kinetics and equilibrium study for the adsorption of textile dyes on coconut shell activated carbon," *Arabian Journal of Chemistry*, vol. 10, pp. S3381–S3393, 2017.

[8] M. W. Ashraf, N. Abulibdeh, and A. Salam, "Adsorption studies of textile dye (chrysoidine) from aqueous solutions using activated sawdust," *International Journal of Chemical Engineering*, vol. 2019, Article ID 9728156, 8 pages, 2019.

[9] V. V. Pathak, R. Kothari, A. K. Chopra, and D. P. Singh, "Experimental and kinetic studies for phycoremediation and dye removal by *Chlorella pyrenoidosa* from textile wastewater,"

Journal of Environmental Management, vol. 163, pp. 270–277, 2015.

[10] P. M. Dellamatrice, M. E. Silva-Stenico, L. A. B. de Moraes, M. F. Fiore, and R. T. R. Monteiro, "Degradation of textile dyes by cyanobacteria," *Brazilian Journal of Microbiology*, vol. 48, no. 1, pp. 25–31, 2017.

[11] C. A. Somensi, E. L. Simionatto, S. L. Bertoli, A. Wisniewski, and C. M. Radetski, "Use of ozone in a pilot-scale plant for textile wastewater pre-treatment: physico-chemical efficiency, degradation by-products identification and environmental toxicity of treated wastewater," *Journal of Hazardous Materials*, vol. 175, no. 1–3, pp. 235–240, 2010.

[12] A. Asghar, A. A. Abdul Raman, and W. M. Ashri Wan Daud, "Advanced oxidation processes for in-situ production of hydrogen peroxide/hydroxyl radical for textile wastewater treatment: a review," *Journal of Cleaner Production*, vol. 87, pp. 826–838, 2015.

[13] L. Bilińska, M. Gmurek, and S. Ledakowicz, "Comparison between industrial and simulated textile wastewater treatment by AOPs–biodegradability, toxicity and cost assessment," *Chemical Engineering Journal*, vol. 306, pp. 550–559, 2016.

[14] R. Liu, H. M. Chiu, R. Y.-L. Shiau, and Y.-T. Hung, "Degradation and sludge production of textile dyes by Fenton and photo-Fenton processes," *Dyes and Pigments*, vol. 73, no. 1, pp. 1–6, 2007.

[15] R. M. Reis, A. A. G. F. Beati, R. S. Rocha et al., "Use of gas diffusion electrode for the in situ generation of hydrogen peroxide in an electrochemical flow-by reactor," *Industrial & Engineering Chemistry Research*, vol. 51, no. 2, pp. 649–654, 2012.

[16] O. Carp, C. L. Huisman, and A. Reller, "Photoinduced reactivity of titanium dioxide," *Progress in Solid State Chemistry*, vol. 32, no. 1-2, pp. 33–177, 2004.

[17] U. G. Akpan and B. H. Hameed, "Parameters affecting the photocatalytic degradation of dyes using TiO_2-based photocatalysts: a review," *Journal of Hazardous Materials*, vol. 170, no. 2-3, pp. 520–529, 2009.

[18] A. J. Attia, S. H. Kadhim, and F. H. Hussein, "Photocatalytic degradation of textile dyeing wastewater using titanium dioxide and zinc oxide," *E-journal of Chemistry*, vol. 5, no. 2, pp. 219–223, 2008.

[19] N. Daneshvar, D. Salari, and A. R. Khataee, "Photocatalytic degradation of azo dye acid red 14 in water on ZnO as an alternative catalyst to TiO_2," *Journal of Photochemistry and Photobiology A: Chemistry*, vol. 162, no. 2-3, pp. 317–322, 2004.

[20] J. Nishio, M. Tokumura, H. T. Znad, and Y. Kawase, "Photocatalytic decolorization of azo-dye with zinc oxide powder in an external UV light irradiation slurry photoreactor," *Journal of Hazardous Materials*, vol. 138, no. 1, pp. 106–115, 2006.

[21] T. Le Thi Thanh, L. Nguyen Thi, T. T. Dinh, and N. Nguyen Van, "Enhanced photocatalytic degradation of Rhodamine B using C/Fe Co-doped titanium dioxide coated on activated carbon," *Journal of Chemistry*, vol. 2019, Article ID 2949316, 8 pages, 2019.

[22] S. Kansal, M. Singh, and D. Sud, "Studies on photodegradation of two commercial dyes in aqueous phase using different photocatalysts," *Journal of Hazardous Materials*, vol. 141, no. 3, pp. 581–590, 2007.

[23] A. Ajmal, I. Majeed, R. N. Malik et al., "Photocatalytic degradation of textile dyes on Cu_2O-CuO/TiO_2 anatase powders," *Journal of Environmental Chemical Engineering*, vol. 4, no. 2, pp. 2138–2146, 2016.

[24] R. Saravanan, M. Mansoob Khan, V. K. Gupta et al., "ZnO/Ag/CdO nanocomposite for visible light-induced photocatalytic degradation of industrial textile effluents," *Journal of Colloid and Interface Science*, vol. 452, pp. 126–133, 2015.

[25] R. Saravanan, E. Sacari, F. Gracia, M. M. Khan, E. Mosquera, and V. K. Gupta, "Conducting PANI stimulated ZnO system for visible light photocatalytic degradation of coloured dyes," *Journal of Molecular Liquids*, vol. 221, pp. 1029–1033, 2016.

[26] C. Piccirillo and P. M. L. Castro, "Calcium hydroxyapatite-based photocatalysts for environment remediation: characteristics, performances and future perspectives," *Journal of Environmental Management*, vol. 193, pp. 79–91, 2017.

[27] M. Sun, D. Li, Y. Chen et al., "Synthesis and photocatalytic activity of calcium antimony oxide hydroxide for the degradation of dyes in water," *The Journal of Physical Chemistry C*, vol. 113, no. 31, pp. 13825–13831, 2009.

[28] M. Kouzu, T. Kasuno, M. Tajika, Y. Sugimoto, S. Yamanaka, and J. Hidaka, "Calcium oxide as a solid base catalyst for transesterification of soybean oil and its application to biodiesel production," *Fuel*, vol. 87, no. 12, pp. 2798–2806, 2008.

[29] https://www.wattagnet.com/articles/36268-latest-poultry-egg-market-forecasts-available-in-2018-watt-poultry-trends.

[30] F. Hamideh and A. Akbar, "Application of eggshell wastes as valuable and utilizable products: a review," *Research in Agricultural Engineering*, vol. 64, no. 2, pp. 104–114, 2018.

[31] A. Mittal, M. Teotia, R. K. Soni, and J. Mittal, "Applications of egg shell and egg shell membrane as adsorbents: a review," *Journal of Molecular Liquids*, vol. 223, pp. 376–387, 2016.

[32] W.-T. Tsai, K.-J. Hsien, H.-C. Hsu, C.-M. Lin, K.-Y. Lin, and C.-H. Chiu, "Utilization of ground eggshell waste as an adsorbent for the removal of dyes from aqueous solution," *Bioresource Technology*, vol. 99, no. 6, pp. 1623–1629, 2008.

[33] M. A. Zulfikar, A. W. Mohammad, and S. Henry, "Adsorption of congo red from aqueous solution using powdered eggshell," *International Journal of Chemtech Research*, vol. 5, no. 4, pp. 1532–1540, 2013.

[34] W. Bessashia, Z. Hattab, Y. Berredjem et al., "Utilization of powdered eggshell waste for rhodamine B removal: evaluation of adsorptive efficiencies and modeling studies," *Sensor Letters*, vol. 16, no. 2, pp. 128–136, 2018.

[35] E. Rápó, R. Szép, A. Keresztesi, M. Suciu, and S. Tonk, "Adsorptive removal of cationic and anionic dyes from aqueous solutions by using eggshell household waste as biosorbent," *Acta Chimica Slovenica*, vol. 65, no. 3, pp. 709–717, 2018.

[36] A. V. Borhade and A. S. Kale, "Calcined eggshell as a cost effective material for removal of dyes from aqueous solution," *Applied Water Science*, vol. 7, no. 8, pp. 4255–4268, 2017.

[37] M. Ehrampoush, G. H. Ghanizadeh, and M. Ghaneian, "Equilibrium and kinetics study of reactive red 123 dye removal from aqueous solution by adsorption on eggshell," *Journal of Environmental Health Science & Engineering*, vol. 8, no. 2, pp. 101–106, 2011.

[38] N. Pramanpol and N. Nitayapat, "Adsorption of reactive dye by eggshell and its membrane," *Kasetsart Journal: Natural Science*, vol. 40, pp. 192–197, 2006.

[39] M. A. El-Kemary, I. M. El-mehasseb, and K. R. Shoueir, "Sol-gel TiO_2 decorated on eggshell nanocrystal as engineered adsorbents for removal of acid dye," *Journal of Dispersion Science and Technology*, vol. 39, no. 6, pp. 911–921, 2018.

[40] M. F. Elkady, A. M. Ibrahim, and M. M. A. El-Latif, "Assessment of the adsorption kinetics, equilibrium and thermodynamic for the potential removal of reactive red dye using

eggshell biocomposite beads," *Desalination*, vol. 278, no. 1–3, pp. 412–423, 2011.

[41] A. S. Yusuff, "Adsorption of cationic dye from aqueous solution using composite chicken eggshell-anthill clay: optimization of adsorbent preparation conditions," *Acta Polytechnica*, vol. 59, no. 2, pp. 192–202, 2019.

[42] M. N. Zafar, M. Amjad, M. Tabassum, I. Ahmad, M. Zubair, and M. Zubair, "$SrFe_2O_4$ nanoferrites and $SrFe_2O_4$/ground eggshell nanocomposites: fast and efficient adsorbents for dyes removal," *Journal of Cleaner Production*, vol. 199, pp. 983–994, 2018.

[43] https://www.britannica.com/technology/calcination.

[44] K. D. Veeranna, M. T. Lakshamaiah, and R. T. Narayan, "Photocatalytic degradation of indigo carmine dye using calcium oxide," *International Journal of Photochemistry*, vol. 2014, Article ID 530570, 6 pages, 2014.

[45] W. T. Tsai, J. M. Yang, C. W. Lai, Y. H. Cheng, C. C. Lin, and C. W. Yeh, "Characterization and adsorption properties of eggshells and eggshell membrane," *Bioresource Technology*, vol. 97, no. 3, pp. 488–493, 2006.

[46] M. El Haddad, A. Regti, M. R. Laamari et al., "Calcined mussel shells as a new and eco-friendly biosorbent to remove textile dyes from aqueous solutions," *Journal of the Taiwan Institute of Chemical Engineers*, vol. 45, no. 2, pp. 533–540, 2014.

[47] D. Yang, T. Fan, Z. Han, J. Ding, and D. Zhang, "Biogenic hierarchical TiO_2/SiO_2 derived from rice husk and enhanced photocatalytic properties for dye degradation," *PLoS One*, vol. 6, no. 9, Article ID e24788, 2011.

[48] A. Houas, H. Lachheb, M. Ksibi, E. Elaloui, C. Guillard, and J.-M. Herrmann, "Photocatalytic degradation pathway of methylene blue in water," *Applied Catalysis B: Environmental*, vol. 31, no. 2, pp. 145–157, 2001.

[49] S. Zhang, "A new nano-sized calcium hydroxide photocatalytic material for the photodegradation of organic dyes," *RSC Advances*, vol. 4, no. 31, pp. 15835–15840, 2014.

[50] F. M. Hossain, G. E. Murch, I. V. Belova, and B. D. Turner, "Electronic, optical and bonding properties of $CaCO_3$ calcite," *Solid State Communications*, vol. 149, no. 29-30, pp. 1201–1203, 2009.

[51] R. Zuo, G. Du, W. Zhang et al., "Photocatalytic degradation of methylene blue using TiO_2 impregnated diatomite," *Advances in Materials Science and Engineering*, vol. 2014, Article ID 170148, 7 pages, 2014.

[52] C. An, S. Peng, and Y. Sun, "Facile synthesis of sunlight-driven AgCl:Ag plasmonic nanophotocatalyst," *Advanced Materials*, vol. 22, no. 23, pp. 2570–2574, 2010.

[53] S. Karagoz, T. Tay, and M. Erdem, "Activated carbons from waste biomass by sulfuric acid activation and their use on methylene blue adsorption," *Bioresource Technology*, vol. 99, no. 14, pp. 6214–6222, 2008.

[54] Y. S. Ho and G. McKay, "Pseudo-second order model for sorption processes," *Process Biochemistry*, vol. 34, no. 5, pp. 451–465, 1999.

[55] N. Madhusudhana, K. Yogendra, and K. M. Mahadevan, "A comparative study on Photocatalytic degradation of Violet GL2B azo dye using CaO and TiO_2 nanoparticles," *International Journal of Engineering Research and Applications*, vol. 2, no. 5, pp. 1300–1307, 2012.